

Synthesis and Characterization of Non-mesogenic Behavior of Chalcone Derivatives

Akmal Alif Awang Mali and Zuhair Jamain*

Organic Synthesis and Advanced Materials (OSAM) Research Group,
Faculty of Science and Natural Resources, Universiti Malaysia Sabah, Jalan UMS,
88400 Kota Kinabalu, Sabah, Malaysia

*Corresponding author (e-mail: zuhairjamain@ums.edu.my)

A series of new chalcone derivatives with different alkyl chain lengths ($C_{10}H_{21}$, $C_{12}H_{25}$, and $C_{14}H_{29}$) have been successfully synthesized and characterized. An initial alkylation reaction of 4-hydroxybenzaldehyde alkyl bromides (decyl, dodecyl, and tetradecyl) formed intermediates **1a**, **1b**, and **1c**, which were further reacted with 4-hydroxyacetophenone through Claisen-Schmidt condensation method to form chalcone derivatives **2a**, **2b**, and **2c**. These compounds were characterized using Fourier Transform Infrared (FTIR) spectroscopy, Nuclear Magnetic Resonance (NMR) spectroscopy, and Carbon, Hydrogen, and Nitrogen (CHN) elemental analysis. The compounds' transition mesophases were determined using Polarized Optical Microscope (POM). However, all the compounds were found non-mesogenic without any liquid crystal properties due to the nonlinearity of the structures.

Keywords: Chalcone; Claisen-Schmidt condensation; liquid crystal; non-mesogenic

Received: September 2022; Accepted: November 2022

Liquid crystals can be classified as an anisotropic material due to the difference in the physical properties of some systems with the average alignment with the director. Increase in a material's alignment causes the compound to exhibit increased anisotropy. Conversely, decrease in the director's arrangement of a material causes the isotropic behavior to be more favorable [1]. This term can be referred to as birefringence, where the light entering a liquid crystal will separate into two linear polarizations with perpendicular directions and different velocities. At low voltages, the soft nature of a liquid crystal medium, along with anisotropic optical and dielectric properties, produces various electro-optic effects, such as dynamic scattering, switchable windows, and light shuttering [2-4]. Increase in voltage causes the polarized refractive index to change, and the director aligns in the direction of the field [5]. Liquid crystal flows act differently than conventional fluids due to the ordered arrangement of the molecules, which can still flow like a liquid [6].

The mesomorphic phase lies between solid crystalline and liquid; thus, the best way to understand the differences is through molecule arrangement [7]. In a solid crystalline state, the molecules are arranged in an order with a repeating pattern for an entire crystal. All the molecules in the crystalline structure are fixed in position through intermolecular forces. These forces become weaker as the molecules vibrate vigorously with the increase in temperature and then causes the molecules to move into a random position [8]. The weaker bonds break when temperature rises because intermolecular forces in solids begin to vibrate

in an uneven direction. As a result, this phenomenon causes a liquid crystal state to form in a random and ordered arrangement [9].

Several properties of liquid crystals can be observed to determine they are liquid crystal compounds. Previous studies showed that liquid crystals exhibit many similarities with isotropic liquid properties except for their molecular units that follow crystalline solids (anisotropic) [10-13]. Viscosity, thermal and electrical conductivity, and optical properties include some of the characteristics that can be determined. Generally, liquid crystals appear cloudy and hazy with a certain degree of order [14].

Thermotropic liquid crystal is the common classification of liquid crystals that exist through thermal process, and they are temperature dependent, which refers to their reaction to temperature changes [15,16]. Generally, temperature will affect the motion of molecules in liquid crystals, which at a very high temperature will convert liquid crystals into isotropic liquids. Conversely, they will become solid crystals as temperature becomes very low to support the thermotropic phase [17]. Specifically, thermotropic liquid crystals can be divided into two groups: enantiotropic liquid crystals and monotropic liquid crystals [18]. Enantiotropic mesophase is a thermodynamically stable state that exists throughout a specific range of temperatures or pressures, contrary to monotropic mesophase, which develops from a cold isotropic liquid. Enantiotropic mesophase's thermal stability is governed by either a liquid crystal compound's melting

and clearing point or by any two subsequent mesophase transitions. Monotropic is a metastable mesophase that forms at a temperature below the melting point of the crystal at a given pressure [19,20].

This research was conducted to explore liquid crystal compounds that had been studied over the years. Nowadays, numerous liquid crystal compounds are being synthesized and analyzed as they grow in interest among researchers and scientists throughout the world. This leads to many new liquid crystal products being discovered and synthesized, such as chalcone derivatives, azo-based compounds, and hydrazine-based compounds. Thus, the discovery of various applications of liquid crystal compounds in daily human life keeps increasing. Specifically for this research, chalcones derivatives have become an interesting field that exhibits various applications in many fields. Benzylideneacetophenone, also commonly known as chalcone, is a compound consisting of two aromatic rings linked by α , β -unsaturated ketone [21]. It can be synthesized in numerous ways, but the most common way is through Claisen-Schmidt condensation using different catalysts. Recently, with an approach to green chemistry, solvent-free chalcone synthesis has been developed [22].

Chalcone is easily found in plants and is one of the main precursors for synthesizing flavonoids. It has been reported that compounds containing chalcone as a backbone have various biological activities such as antimicrobial, anti-inflammatory, antiplatelet, anti-malarial, anticancer, antiviral, and antihyperglycemic [23-25]. The reactive and unsaturated keto groups, especially for antimicrobial activity, are the key functional groups responsible for all these activities [26]. Besides that, chalcone derivatives also play an important role in crystallography, liquid crystalline polymers, dye industries, and solar cells. However, the potential of chalcones and recent updates are few and need to be understood. Hence, explaining the structure, purpose, and mesophase behavior of synthesizing new chalcone derivatives is to maximize the application of liquid crystals, especially for chalcone compounds in the future.

EXPERIMENTAL

Chemicals and Materials

The chemicals and solvents used in this study were 4-hydroxybenzaldehyde, 4-hydroxyacetophenone, 1-bromodecane, 1-bromododecane, 1-bromotetradecane, potassium carbonate, potassium iodide, sodium hydroxide, *N,N*-dimethylformamide (DMF), dichloromethane (DCM), hydrochloric acid, ethanol, and methanol. All the chemicals were used as received

without purification and were purchased from Merck, Qręc, Sigma-Aldrich, Across, and BDH laboratory.

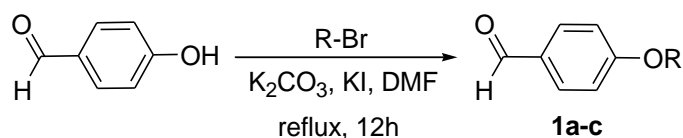
Characterization Methods

In this study, Fourier-Transform infrared (FTIR) spectroscopy was used to determine the functional groups observed in the chalcone derivatives, such as the ketone and phenyl functional groups. Besides, nuclear magnetic resonance (NMR) spectroscopy was used to determine the structure and conformation of chalcone moiety in the derivatives. Carbon, hydrogen, and nitrogen (CHN) elemental analyzers were used to determine the purity of chalcone derivatives that show the amounts of carbon, hydrogen, and nitrogen since chalcone compounds are an organic matrix. The texture of the mesophase of the compounds was observed using Polarized Optical Microscope (POM). The samples were sandwiched between two round glass slides placed on the microscope's hot stage. The microscope was adjusted to obtain a clear resolution, and the phase transitions were observed in the heating and cooling cycles.

Synthesis Methods

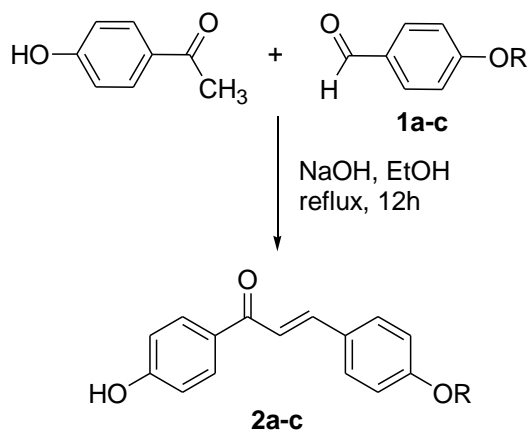
New chalcone derivatives were synthesized through a method called Claisen-Schmidt condensation, which involves the condensation of 4-(alkoxy)benzaldehyde with acetophenone under an aqueous alkali (NaOH). 4-(alkoxy)benzaldehyde was synthesized through alkylation reaction. In the first step, a base, potassium carbonate (K_2CO_3), is used to extract hydrogen from the hydroxyl group and alkoxide ion. In the second step, the alkoxide ion acts as a nucleophile and attacks the carbon bonded to the halogen group of 1-bromodecane through SN2 mechanism to form the intermediate 4-(alkoxy)benzaldehyde.

Next, new chalcone derivatives were formed by reacting the first intermediate with 4-hydroxyacetophenone through Claisen-Schmidt condensation. This reaction was done in the presence of a basic catalyst, sodium hydroxide (NaOH). The base extracts the α -hydrogen from 4-hydroxyacetophenone, and an enolate ion is the product. The enolate ion is then stabilized by resonance. The double bond electrons then attack the carbonyl carbon of the first intermediate, followed by the abstraction of H^+ ions from water and gives rise to the aldol compound. This aldol compound would then undergo a dehydration process catalyzed by hydroxide ions. This hydroxide ion will attack the α -hydrogen, followed by the expulsion of hydroxide at β -carbon. A double bond is then formed between α and β carbons. The general synthesis methods of the intermediates [27] and chalcone derivatives [28,29] are illustrated in Schemes 1-2.



R = C₁₀H₂₁, **1a**; C₁₂H₂₅, **1b**; C₁₄H₂₉, **1c**

Scheme 1. Alkylation reaction. Synthesis of intermediates **1a-c**



R = C₁₀H₂₁, **2a**; C₁₂H₂₅, **2b**; C₁₄H₂₉, **2c**

Scheme 2. Claisen-Schmidt condensation reaction. Synthesis of compounds **2a-c**

Synthesis of 4-alkoxybenzaldehyde Intermediates **1a-c**

0.1 mol of 4-hydroxybenzaldehyde and 0.1 mol of 1-bromoheptane were dissolved in 20 mL of *N,N*-dimethyl formamide (DMF), separately. The solutions were then mixed in a 250 mL round bottom flask. 0.15 mol of potassium carbonate and 0.01 mol of potassium iodide were added and the mixture was refluxed for 12 hours. The reaction progress was monitored using thin layer chromatography (TLC). Next, the mixture was poured into 500 mL of cold water and extracted using dichloromethane. The organic layer was collected and dried in anhydrous sodium sulphate. The product, intermediate **1a**, was filtered and evaporated overnight. The same procedure was used to synthesize **1b-c**.

4-(decyloxy)benzaldehyde, **1a**. Yield = 2.51 g (95.80%), dark yellow oil. IR (cm⁻¹): 2848 and 2733 (CHO stretching), 1691 (C=O aldehyde), 1600 and 1509 (aromatic C=C stretching), 1250 and 1167 (C-O stretching). ¹H NMR (500 MHz, CDCl₃) δ, ppm: 9.71 (s, 1H), 7.65 (d, *J* = 5.15 Hz, 2H), 6.82 (d, *J* = 5.15 Hz, 2H), 3.84 (t, *J* = 2.9 Hz, 2H), 1.59-1.64 (m, 2H), 1.13-1.31 (m, 14H), 0.75 (t, *J* = 3.45 Hz, 3H). ¹³C NMR (125 MHz, CDCl₃) δ, ppm: 190.23, 164.18, 131.82, 129.73, 114.65, 68.31, 31.90, 29.58, 29.35, 25.97, 22.68, 14.09.

4-(dodecyloxy)benzaldehyde, **1b**. Yield = 2.86 g (98.62%), light yellow oil. IR (cm⁻¹): 2853 and 2731

(CHO stretching), 1692 (C=O aldehyde), 1599 and 1508 (aromatic C=C stretching), 1254 and 1157 (C-O stretching). ¹H NMR (500 MHz, CDCl₃) δ, ppm: 9.77 (s, 1H), 7.72 (d, *J* = 7.45, 2H), 6.89 (d, *J* = 7.4, 2H), 3.93 (t, *J* = 5.15, 2H), 1.72 (m, 2H), 1.31-1.39 (m, 2H), 1.20-1.28 (m, 14H), 0.81 (t, *J* = 5.75). ¹³C NMR (125 MHz, CDCl₃) δ, ppm: 190.65, 164.29, 131.96, 129.78, 114.75, 68.42, 31.98, 29.66, 29.11, 26.03, 22.75, 14.17.

4-(tetradecyloxy)benzaldehyde, **1c**. Yield = 311.54 g (97.88%), mp: 56.6 °C - 58.7°C, white powder. IR (cm⁻¹): 2853 and 2731 (CHO stretching), 1690 (C=O aldehyde), 1599 and 1508 (aromatic C=C stretching), 1253 and 1157 (C-O stretching). ¹H NMR (500 MHz, CDCl₃) δ, ppm: 9.81 (s, 1H), 7.76 (d, *J* = 6.45, 2H), 6.93 (d, *J* = 6.45, 2H), 3.96 (t, *J* = 5.15, 2H), 1.74 (m, 2H), 1.31-1.36 (m, 2H), 1.13-1.29 (m, 16H), 0.88 (t, *J* = 5.75, 3H). ¹³C NMR (125 MHz, CDCl₃) δ, ppm: 190.65, 164.29, 131.96, 129.78, 114.75, 68.42, 31.98, 29.66, 29.11, 26.03, 22.75, 14.17. CHN elemental analysis: Calculated for C₂₁H₃₄O₂: C: 79.19%, H: 10.76%; Found: C: 81.20%, H: 10.49%.

Synthesis of Compounds **2a-c**

0.10 mol of 4-hydroxyacetophenone and 0.10 mol of intermediate **1a** were added into a round bottom flask containing 500 mL of ethanol. The mixture was then stirred in an ice bath. NaOH was added dropwise and

the mixture was left for 30 minutes. Then, the mixture was refluxed for 12 hours under constant stirring. The resultant mixture was left to cool and neutralized using ice chilled dilute HCl (5%). The precipitate was filtered and washed with ice cold distilled water until it was free from acid. Recrystallization of the compound, **2a**, was done using methanol. The same procedure was used to synthesize **2b-c**.

(E)-3-(4-(decyloxy)phenyl)-1-(*p*-tolyl)prop-2-en-1-one, **2a**. Yield = 3.44g (91.01%), mp: 81.7-82.1°C, dark yellow powder. IR (cm⁻¹): 2923 and 2853 (Csp³-H stretching), 1688 (C=O keto), 1598 and 1509 (aromatic C=C stretching), 1254 and 1157 (C-O stretching). ¹H NMR (500 MHz, CDCl₃) δ, ppm: 8.03 (d, *J* = 10, 2H), 7.08 (d, *J* = 10, 2H), 7.08 (d, *J* = 10, 2H), 6.91 (d, *J* = 10, 2H), 6.60 (d, *J* = 5, 2H), 6.60 (d, *J* = 5, 2H), 4.00 (t, *J* = 5, 2H), 1.44 (s, 3H), 1.76 – 1.81 (m, 2H), 1.26-1.41 (m, 14H), 0.83 (t, *J* = 10, 3H). ¹³C NMR (125 MHz, CDCl₃) δ, ppm: 190.03, 171.55, 163.68, 144.76, 140.06, 132.32, 129.13, 123.36, 121.40, 116.36, 114.31, 68.31, 31.87, 29.51, 29.36, 29.25, 29.10, 29.10, 25.98, 22.67, 14.10. CHN elemental analysis: Calculated for C₂₆H₃₄O₂: C: 82.49%, H: 9.05%; Found: C: 81.20%, H: 9.29%.

(E)-3-(4-(dodecyloxy)phenyl)-1-(*p*-tolyl)prop-2-en-1-one, **2b**. Yield = 3.62g (89.10%), mp: 79.8-80.7°C, light yellow powder. IR (cm⁻¹): 2923 and 2853 (Csp³-H stretching), 1690 (C=O keto), 1599 and 1509 (aromatic C=C stretching), 1255 and 1157 (C-O stretching). ¹H NMR (500 MHz, CDCl₃) δ, ppm: 8.04 (d, *J* = 5, 2H), 7.78 (d, *J* = 15.60, 2H), 7.41 (d, *J* = 15.12, 2H), 7.08 (d, *J* = 10, 2H), 6.92 (d, *J* = 5, 2H), 6.59 (d, *J* = 10, 2H), 4.02 (t, *J* = 5, 2H), 1.35 (s, 3H), 1.77-1.82 (m, 2H), 1.28-1.49 (m, 14H), 0.88 (t, *J* = 5, 3H). ¹³C NMR (125 MHz, CDCl₃) δ, ppm: 191.11, 171.51, 163.73, 144.71, 130.01, 132.29, 129.11, 123.49, 121.53, 116.38, 114.26, 68.35, 31.87, 29.60, 29.58, 29.53, 29.50, 29.30, 29.28, 29.09, 29.09, 25.95, 22.61, 13.98. CHN elemental analysis: Calculated for C₂₈H₃₈O₂: C: 82.71%, H: 9.42%; Found: C: 80.87%, H: 9.21%.

(E)-3-(4-(tetradecyloxy)phenyl)-1-(*p*-tolyl)prop-2-en-1-one, **2c**. Yield = 4.06g (93.5%), mp: 75.7-77.6°C, white powder. IR (cm⁻¹): 2915 and 2848 (Csp³-H stretching), 1691 (C=O keto), 1600 and 1509 (aromatic C=C stretching), 1256 and 1166 (C-O stretching). ¹H NMR (500 MHz, CDCl₃) δ, ppm: 8.04 (d, *J* = 5, 2H), 7.78 (d, *J* = 15.60, 2H), 7.41 (d, *J* = 15.12, 2H), 7.08 (d, *J* = 10, 2H), 6.92 (d, *J* = 5, 2H), 6.59 (d, *J* = 10, 2H), 4.02 (t, *J* = 5, 2H), 1.35 (s, 3H), 1.77-1.82 (m, 2H), 1.28-1.49 (m, 14H), 0.88 (t, *J* = 5, 3H). ¹³C NMR (125 MHz, CDCl₃) δ, ppm: 190.03, 171.11, 163.75, 144.73, 140.03, 132.25, 129.09, 123.53, 121.59, 116.37, 114.30, 68.38, 31.83, 29.55, 29.53, 29.51, 29.48, 29.46, 29.45, 29.26, 29.23, 29.09, 25.93, 22.56, 13.88. CHN elemental analysis: Calculated for C₃₀H₄₂O₂: C: 82.90%, H: 9.74%; Found: C: 84.31%, H: 9.21%

RESULTS AND DISCUSSION

FTIR Spectral Discussion of Compounds **2a-c**

FTIR analysis of final compound **2a** as the representative of compounds **2b** and **2c** was carried out to identify the various functional groups in these compounds. In the FTIR spectrum, two peaks in the range of 2800 to 3000 cm⁻¹ were observed, which were at wave numbers 2923.01 and 2853.30 cm⁻¹, specifically assigned as the C-H stretching vibrations of methyl and methylene. Thus, the C-H stretch could be confirmed by observing the low frequency ranged from 1350 to 1500 cm⁻¹ and the presence of peaks could be noticed at wave numbers 1466.93 cm⁻¹ and 1393.51 cm⁻¹, which strongly indicate the presence of methyl group or to be specific the existence of the bending of -CH₂ and -CH₃ (symmetric), respectively in the alkyl chain within the intermediates. Hence, the existence of alkane groups in the intermediates is confirmed by these regions of the absorption spectra.

The next peak observed was at 1690.08 cm⁻¹. From its intensity and position, it could be assigned as a carbonyl, C=O stretching vibration. However, as mentioned earlier, this band could not indicate to which specific carbonyl group it belonged to. This band could be aromatic ketone, aromatic acid, or an amide. Therefore, it can be confirmed that this peak belonged to ketone group as there was no low wave number C-H stretch near 2750 cm⁻¹ that indicates the CHO stretch. Thus, this compound is not an aldehyde. Plus, this compound is not an acid too because there was no strong O-H stretching vibration near 3400 cm⁻¹ and it is not an ester because it did not have the rule of three bands. Moreover, the exact position of this C=O shifted to a lower frequency under conjugation effect as it was presented adjacent to an unsaturated benzene ring. This results in delocalization of π electrons in C=O and C=C bonds in the aromatic ring. This conjugation increases the single-bond character of the C=O and C=C bonds in resonance hybrid, hence, lowers their force constant, resulting in a lowering of frequency of C=O absorption. Therefore, compound **2a** was suggested as an acetophenone, in which an aryl group was attached to the carbonyl group.

The C=C stretching bands for aromatic rings usually appear in the range of 1600 to 1450 cm⁻¹. There are usually sharp bands near 1600, 1500 and 1475 cm⁻¹ in benzene. These three peaks could be observed in the spectral data at 1599.34, 1576.81, and 1509.22 cm⁻¹, respectively. They were the C=C stretches in benzene ring of ring stretch. The substitution pattern on the aromatic ring can be determined by observing the peak at wave number 831.35 cm⁻¹, which are the out-of-plane and aromatic ring-bending modes. The band indicated that all the final compounds had para-disubstituted (1,4-disubstituted) ring in the structure.

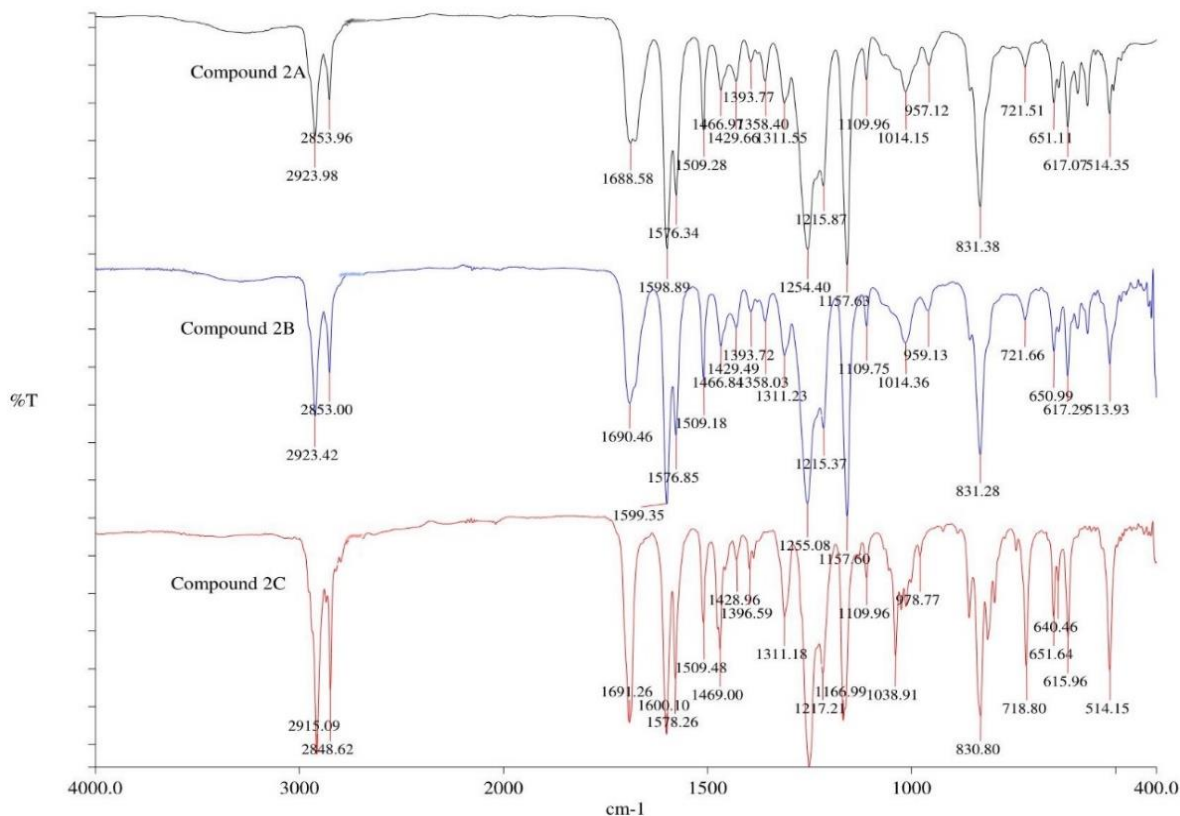


Figure 1. Overlay FTIR spectra of compounds **2a-c**

There were a series of four sharp and intense peaks observed at 1255.15, 1157.71, 1109.88, and 1015.10 cm^{-1} , which are assigned to C-O stretch in ether. The intermediate was confirmed as ether and not phenol of alcohol because there was the absence of O-H stretching region near 3400 cm^{-1} .

Figure 1 shows the overlay FTIR spectra for all the final compounds. It can be concluded that the value for all the wave numbers together with the peak intensities were almost the same. This is because final compounds **2a**, **2b** and **2c** have the same functional groups with different lengths of alkyl chains attached to them. Although the FTIR spectral data of the final compounds were almost the same as the intermediates, it could be observed that the significant difference between the two sets of spectral data is the elimination peak near 2750 cm^{-1} in the FTIR spectral data for the final compounds, hence indicates the absence of the aldehyde group in the final compounds. This can also

confirm that the presence of the ketone carbonyl group in the final compounds instead of the aldehyde group.

NMR Spectral Discussion of Compounds **2a-c**

¹H NMR Spectral Discussion

The structure of (E)-3-(4-(decyloxy)phenyl)-1-(p-tolyl)prop-2-en-1-one, compound **2a** (Figure 2), with complete atomic numbering was used to represent the other homologues.

The ¹H NMR spectrum of compound **2a** is shown in Figure 3. The significant difference of signal for the final compounds compared to the intermediates was the absence of signals in the range of $\delta = 9.00 - 10.00$ ppm, which indicates the RCHO of the aldehyde group. Multiplet signals present in the region of $\delta = 8.04 - 6.59$ ppm are assigned as the aromatic protons (ArH). Doublet signals present at $\delta = 7.08$ ppm are

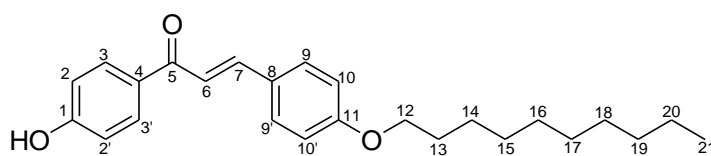


Figure 2. Structure of compound **2a** with complete atomic numbering

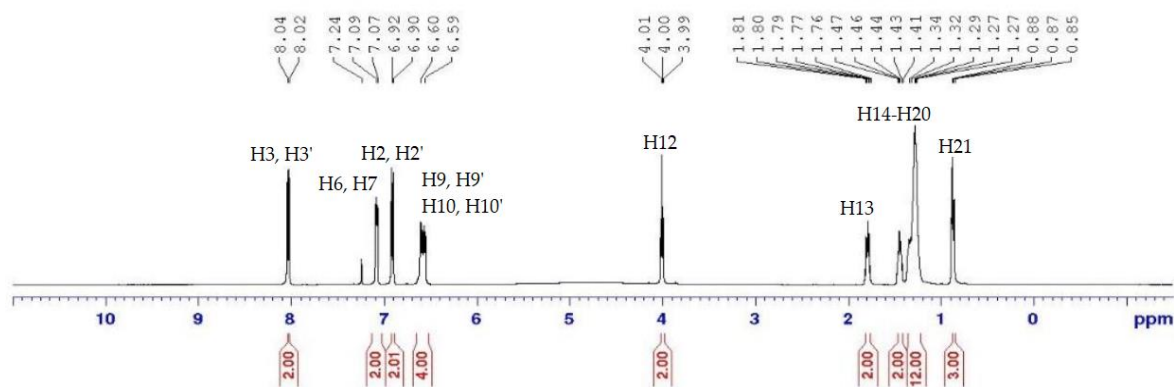


Figure 3. ^1H (500 MHz, CDCl_3) NMR spectrum of compound **2a**

assigned as the olefinic protons. Protons in the $-\text{O}-\text{CH}_2-$ group were found at $\delta = 4.00$ ppm, and the following proton on the next carbon atom in the alkyl chain had a chemical shift of $\delta = 1.78$ ppm. The remaining protons in the alkyl chain were found in the region of $\delta = 1.26 - 1.41$ ppm. Protons of the methyl group were found at $\delta = 0.83$ ppm.

The carbonyl group was directly attached to the phenyl group *para* to H3 and H3', thus this electron withdrawing group underwent conjugation with the phenyl group. The resulting resonance formed would have a lower electron density at *ortho* and *para* positions of the phenyl group. Besides that, the magnetic anisotropy effect caused by π -bond of carbonyl to the *para* position further deshielded the *para* protons. This then led to H3 and H3' signals appearing at the deshielded region due to lower electron density around these protons. Similar reasons could be applied to the deshielding effect of H2 and H2'. H2 and H2' were slightly further away from the carbonyl group, thus the deshielding effect was lower compared to H3 and H3'. H9, H9', H10, and H10' signals appeared as two doublets at $\delta = 6.60$ ppm and these four protons belonged to Ar-H. These four protons appeared at a more shielded region compared to H2, H2', H3, and H3'. This is due to these four protons being further away from the carbonyl group, thus the inductive effect was not as strong as the resonance effect but the electron donation effect from oxygen of ether increased the electron density around these H9 and H9' protons, causing them to appear at a slightly more shielded region. The coupling constant for H2, H2' and H3, H3' was the same, which was 10. Based on calculated coupling constant, it is suggested that the interaction between H2 and H2' with H3 and H3' is *para* interaction. Similar reasons were applied to H9, H9' and H10, H10', which have the same value of coupling constant of $J = 5$.

The olefinic protons found at the downfield region ($\delta = 7.08$ ppm) were assigned to the α -position (H7) and β -position (H6) of unsaturated ketone due to

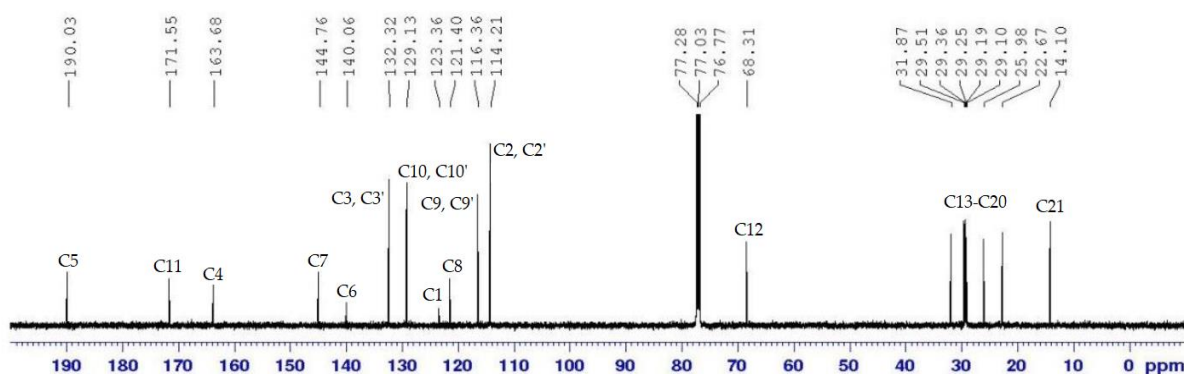
the resonance formed by α, β -unsaturated ketone. According to the theory, the β -carbon and β -hydrogen were more deshielded because of the lower electron density around the β -carbon. Besides that, the anisotropic field generated by the π -electrons of benzene would interact with the β -hydrogen, which further deshield it. In addition, it was found that H7 coupled with H6 show doublet with coupling constant of $J_{5,4} = 10$ Hz. These values of coupling constant between H6 and H7 suggest that the interactions between these two protons were in *trans* position.

H12 signal appeared at a moderately shielded region ($\delta = 4.00$ ppm). The electron density around it was highly dense although these protons were directly attached to the oxygen of ether. This is due to the donation effect from the alkyl chain. The electron withdrawing effect of ether's oxygen was reduced due to the donation effect from the alkyl chain, therefore, even with the presence of oxygen attached directly to the carbon bonded to H12, the electron density around H12 remained dense and the signal appeared at a moderately shielded region. Besides that, the oxygen of the ether group can act as electron donating group, thus further increases the electron density around H12.

Signals at $\delta = 1.26 - 1.81$ ppm represented the protons in the alkyl chain (H13 - H20). They appeared at highly shielded regions as the electron densities of the protons were very high. A signal (H21) was observed at $\delta = 0.83$ ppm and this signal represented methyl group of alkyl chain, and it was the furthest from the benzene or carbonyl group, thus it was the most downfield signal. For this compound, there was no electron withdrawing group attached directly to it, thus the electron density was highly dense. The NMR spectra for **2b** and **2c** have almost the same pattern as the discussed **2a** NMR spectral data, but with a slight difference especially in the range of $\delta = 1.0 - 2.0$ ppm, as **2b** and **2c** have longer alkyl chains compared to **2a**. All the data of chemical shift, δ (ppm), coupling constant (J) and multiplicity of compound **2a** are tabulated in Table 1.

Table 1. ^1H NMR data summary of compound **2a**

Proton(s)	Number(s) of H	Coupling constant, J (Hz)	Chemical shift, ppm	Multiplicity of signal(s)
H2 & H2'	2	10	6.91	d
H3 & H3'	2	10	8.03	d
H6	1	10	7.08	d
H7	1	10	7.08	d
H9 & H9'	2	5	6.60	d
H10 & H10'	2	5	6.60	d
H12	2	5	4.00	t
H13	2	-	1.76 – 1.81	m
H14 – H20	14	-	1.26-1.41	m
H21	3	5.75	0.83	t

**Figure 4.** ^{13}C (125 MHz, CDCl_3) NMR spectrum of compound **2a**

^{13}C NMR Spectral Discussion

Figure 4 was used for the assignment of carbon signals in compound **2a**. Solvent peak at $\delta = 77.11$ ppm represented CDCl_3 , as demonstrated in Figure 4. Carbonyl carbon was assigned at $\delta = 197.82$ ppm. Aromatic carbon peaks were within $\delta = 171.55 - 114.21$ ppm. Ether carbon was at $\delta = 68.31$ ppm, while other signals represented aliphatic carbon.

C5 was found in the most deshielded region in the ^{13}C NMR spectrum due to the highly electronegative oxygen atom directly attached to the carbon of the carbonyl group of ketones. Oxygen has electron withdrawing properties, thus it withdraws the electron density away from carbon toward itself. Therefore, the carbon of the carbonyl group has low electron density which causes it to be deshielded. In addition, the magnetic anisotropy effect generated by phenyl and olefin π electrons further deshields the carbonyl carbon. The signal at $\delta = 144.76$ ppm was assigned to C7 due to its more electron poor characteristic as β -carbon in α,β -unsaturated ketone. Through the resonance of α,β -unsaturated ketone, the electron density on the β -carbon would be pulled towards the carbonyl group, thus making it highly deshielded compared to α -carbon. Through this resonance structure, α -carbon will be more shielded than β -

carbon, thus its signal appeared at $\delta = 140.06$ ppm. Another possible reason of lower electron density on β -carbon is due to anisotropic field generated by π electrons of phenyl group.

The region of $\delta = 171.55 - 114.00$ ppm was assigned to Ar-C. It could be further classified whereby C4 and C1 signals were at $\delta = 163.68$ and 123.36 ppm; C8 and C11 at $\delta = 121.40$ and 171.55 ppm; and C2, C3, C9, and C10 at $\delta = 114.21$, 132.32, 116.36, and 129.13 ppm, respectively. The assignment of signals could be done by observing the intensity of the carbon signals in the ^{13}C NMR spectrum.

Next, the signal (C12) at $\delta = 68.31$ represented the ether bond present in the compound. The carbon directly attached to the oxygen is slightly deshielded but not as highly deshielded as the carbon of the carbonyl group due to electron donation effect of oxygen atom. Therefore, carbon bonded to oxygen through ether bond has higher electron density and the signal appears at moderately shielded region. It was observed that many signals were present in the region of $\delta = 25.98 - 31.87$ ppm and these signals represented the alkyl chain (C13 – C20). It was found that all the signals gave similar abundance. The most downfield carbon signal (C21) of the methyl group in the alkyl chain was found to at $\delta = 14.10$ ppm.

Table 2. ^{13}C NMR data summary of compound **2a**

Position of C	Chemical Shift (ppm)
C1	123.36
C2 & C2'	114.21
C3 & C3'	132.32
C4	163.68
C5	190.03
C6	140.06
C7	144.76
C8	121.40
C9 & C9'	116.36
C10 & C10'	129.13
C11	171.55
C12	68.31
C13	31.87
C14-C20	25.98 – 29.51
C21	14.10

The NMR spectra for **2b** and **2c** have almost the same pattern as **2a**, but with a slight difference especially in the range of $\delta = 20.0\text{-}35.0$ ppm, as **2b** and **2c** have longer alkyl chains attached to them that will cause more signals to appear in that region according to the increasing number of carbons of the alkyl chains from **2b** and **2c**. The assignment of carbon signals in compound **2a** is summarized in Table 2.

CHN Elemental Analysis

The percentages of carbon (C), hydrogen (H), and nitrogen (N) of compounds **1c**, **2a**, **2b**, and **2c** are summarized in Table 3. The percentage error for each compound characterized was less than 3%,

indicating that all compounds synthesized were pure.

Determination of Liquid Crystal Properties

Determination of mesophase(s) behavior for all compounds was done using polarized optical microscope (POM). The texture of phase transitions can be seen in a sample that has been placed under a microscope at a controlled temperature. An average of 5-10 mg of samples was used, and the temperature was scanned at the rate of 5 °C/min. All the data are summarized in Table 4. However, all the synthesized compounds were found to be non-mesogenic without liquid crystal properties.

Table 3. CHN elemental analysis data of compounds **1c**, **2a**, **2b**, and **2c**

Compound	% Found (Calculated)		
	C (%)	H (%)	Percentage error (%)
1c	81.20 (79.19)	10.49 (10.76)	2.54
2a	82.49 (81.20)	9.05 (9.29)	1.54
2b	82.71 (80.87)	9.42 (9.21)	2.24
2c	82.90 (84.31)	9.74 (9.21)	1.74

Table 4. Phase sequence of compounds **2a-c**

Compound	Mode	Transition Temperature
2a	Heating	Cr → I 82.1 °C
	Cooling	I → Cr 81.7 °C
2b	Heating	Cr → I 80.7 °C
	Cooling	I → Cr 79.8 °C
2c	Heating	Cr → I 77.6 °C
	Cooling	I → Cr 75.7 °C

Based from Table 4, the new series of chalcone derivatives do not exhibit liquid crystal mesophase, whether in heating or cooling cycles. All these compounds underwent direct isotropization process and directly formed a clear isotropic liquid instead of going through liquid crystalline phases. Among these three compounds, **2a** has the highest melting point while **2c** has the lowest melting point. This might be due to the decrease of van der Waal forces among compounds **2a-c**. Cohesive forces are increase with the increasing of the chain length at the terminal chain, thus more energy is required to break these bonds, which leads to higher melting point [30,31]. But still, the elongated structure of these chalcone derivatives do not exhibit any liquid crystal phase.

Terminal substituents can attract and repel one another in different molecules and affect the polarizability of the aromatic rings to which they are attached [32]. In addition, terminal substituents may interact with the lateral portion of an adjacent molecule. Substituents are chosen to cover a wide range of steric and electronic nature, representing the conjugated interaction with the central linking group via the intervening benzene rings. The terminal groups include the length of the terminal chains (alkyl or alkoxy) and the intermolecular interactions due to the coordinated oxygen atom [33]. Longer terminal chains lower the melting points and widen the range of liquid crystal mesophases [34,35]. The alkyl length controls the stability of the mesophase. Compounds with long alkyl chains exhibit enantiotropic mesophase which is thermodynamically stable, while compounds with shorter alkyl chains show monotropic mesophase which has unstable behavior [36].

In a nutshell, the new series of chalcone derivatives having enone (-CH=CH-CO-) group as a central linkage do not exhibit liquid crystal phase. This might be due to the enone group which has odd number atoms, thus is less conducive to mesomorphism compared even number linkages. It is unfavorable to mesomorphism due to non-linearity which is against the main principle of liquid crystalline phase that

needs to have a linear molecular axis [37]. In addition, there were less electronegativity atoms attached, which leads to low polarizability of the compounds [38]. Besides that, the angular shape of keto group causes angle strain in the linking group, which makes all chalcone derivatives less prone in exhibiting liquid crystalline phase [39,40].

CONCLUSION

A series of new chalcone derivatives, (E)-3-(4-(alkoxy) phenyl)-1-(p-tolyl)prop-2-en-1-one, with decyloxy, dodecyloxy and tetracyloxy terminal chains have been successfully synthesized and characterized. The functional groups of all the compounds were identified using Fourier Transform Infrared (FTIR) spectroscopy, while their molecular structures were confirmed by Nuclear Magnetic Resonance (NMR) spectroscopy. The purity of these compounds was confirmed using CHN elemental analysis. Polarized Optical Microscopy (POM) was used to determine the liquid crystal properties of the synthesized compounds. Observations under POM showed that none of these compounds exhibit mesomorphic properties. The possible reason is the nonlinearity, which is caused by the enone group in chalcone moiety and thus making it less conducive to mesomorphism. There were less electronegativity atoms attached, which led to low polarizability of the compounds. Moreover, the angular shape of keto group causes angle strain in the linking group, which makes all chalcone derivatives less prone in exhibiting liquid crystalline phase. Hence, future studies of chalcone derivatives could be done by introducing an additional linkage of the phenyl ring to the chalcone. Even though the enone group is not conducive to mesomorphism, it can be changed by including other central linkages such as azomethine, ester or azo groups. The addition of electronegative atoms and phenyl rings to the structure is suggested to enhance the liquid crystalline properties as it increases the polarizability of the molecules. The finding of liquid crystal materials occupies a specific place among other organic compounds used in electronics, laser technique, solar energy, and biomedicine. It

relates to their anisotropic parameters activated by electric, magnetic, thermal, acoustic, etc. Thus, the understanding in a structure-property relationship is important to produce LC compounds with specific functionality.

ACKNOWLEDGEMENT

The authors would like to thank Universiti Malaysia Sabah (UMS) for the financial support (grant numbers SBK0488-2021 and SPB0004-2020) and technical support.

REFERENCES

1. Andrienko, D. (2018) Introduction to Liquid Crystals. *Journal of Molecular Liquids*, **267**, 520–541.
2. Al-Karawi, A. J. M., Hammood, A. J., Awad, A. A., Omar Ali, A. A. B., Khudhaier, S. R., Al-Heetimi, D. T., Majeed, S. G. (2018) Synthesis and mesomorphism behaviour of chalcones and pyrazoles type compounds as photo-luminescent materials. *Liquid Crystals*, **45**, 1603–1619.
3. Zhang, Y., Zhao, Y., Lv, R. (2015) A review for optical sensors based on photonic crystal cavities. *Sensors and Actuators A: Physical*, **233**, 374–389.
4. Okubo, T., Tsuchida, A., Stoimenova, M. (2011) Electro-optic effects of colloidal crystals. *Advances in Colloid and Interface Science*, **162**, 80–86.
5. Goodman, L. A. (1975) Liquid-Crystal Displays—Electro-Optic Effects and Addressing Techniques. In: Priestley, E.B., Wojtowicz, P.J., Sheng, P. (eds) Introduction to Liquid Crystals. Springer, Boston, MA. <https://doi.org/10.1007/978-1-4684-2175-014>
6. Collings, P. J. (2002) Liquid Crystals: Nature's Delicate Phase of Matter; Princeton University Press: Princeton, NJ, USA.
7. Bukowczan, A., Edyta Hebda, E., Pielichowski, K. (2021) The influence of nanoparticles on phase formation and stability of liquid crystals and liquid crystalline polymers. *Journal of Molecular Liquids*, **321**, 114849.
8. Jamain, Z., Khairuddean, M., Kamaruddin, N. K., Rui, Y. Z. (2021) Synthesis, structural elucidation and mesophase behaviour of hexa-substituted cyclotriphosphazene molecules with amide linking unit. *Malaysian Journal of Chemistry*, **23**, 213–225.
9. Jeong, M. J., Park, J. H., Lee, C., Chang, J. Y. (2006) Discotic liquid hydrazone compounds: Synthesis and mesomorphic properties. *Organic Letters*, **8**, 2221–2224.
10. Dixit, S., Intwala, K. (2016) Study of novel thermotropic liquid crystals with lateral nitro substituent. *Liquid Crystals*, **631**, 1–8.
11. Irina, C., Ana M. S., Daniela, A., Valentina, A., Dan, S. (2007) The liquid crystalline behaviour of ferrocene derivatives containing azo and imine linking groups. *Liquid Crystals*, **34**, 775–785.
12. Issam, A. A., Sankar, G., Khairuddean, M., Mohamad, A. A. (2010) Synthesis and liquid crystalline properties of new diols containing azomethine groups. *Molecules*, **15**, 3260–3269.
13. Razali, N. A., Jamain, Z. (2021) Liquid crystals investigation behavior on azo-based compounds: A review. *Polymers*, **13**, 3462.
14. Javed, A., Akram, M., Shafiq, M. I. (2006) Dielectric properties of cholesterol derivatives. *Romanian Journal of Physics*, **51**, 819.
15. Jamain, Z., Khairuddean, M., Saidin, S. A. (2019) Synthesis and characterization of 1,4-phenylene-diamine derivatives containing hydroxyl and cyclotriphosphazene as terminal group. *Journal of Molecular Structure*, **1186**, 293–302.
16. Jamain, Z., Omar, N. F., Khairuddean, M. (2020) Synthesis and determination of thermotropic liquid crystalline behavior of cinnamaldehyde-based molecules with two Schiff base linking units. *Molecules*, **25**, 3780.
17. Bagheri, M., Rad, R. Z. (2007) Synthesis and characterization of thermotropic liquid crystalline polyesters with biphenyl unit in the main chain. *Reactive and Functional Polymers*, **68**, 613–622.
18. Mandle, R. J., Cowling, S. J., Goodby, J. W. (2017) A nematic to nematic transformation exhibited by a rod-like liquid crystal. *Physical Chemistry Chemical Physics*, **19**, 11429–11435.
19. Collings, P. J., Hird, M. (1997) Introduction to Liquid Crystal, Chemistry and Physics; Taylor & Francis: London, UK.
20. Devi, K.; Bharracharjee, A. (2010) A Review of Liquid Crystal Dimers. *Assam University Journal of Science & Technology: Physical Sciences and Technology*, **5**, 225–228.
21. Song, D. M., Jung, K. H., Shin, D. M. (2002) Photochemical behavior of chalcone and the photo-alignment of liquid crystals with chalcone derivatives. *Molecular Crystals and Liquid Crystals*, **337**, 117–120.
22. Kumar, D., Suresh, Sandhu, J. S. (2010) An efficient green protocol for the synthesis of chalcones by a Claisen-Schmidt reaction using

- bismuth(III)chloride as a catalyst under solvent-free condition. *Green Chemistry Letters and Reviews*, **3**, 283–286.
23. Sahu, N. K., Balbhadra, S. S., Choudhary, J., Kohli, D. V. (2012) Exploring pharmacological significance of chalcone scaffold: A review. *Current Medicinal Chemistry*, **19**, 209–225.
 24. Ngaini, Z., Fadzillah, S. M. H., Hussain, H. (2012) Synthesis and antimicrobial studies of hydroxylated chalcone derivatives with variable chain length. *Natural Product Research*, **26**, 892–902.
 25. Wijayanti, L. W., Swasono, R. T., Lee, W., Jumina, J. (2020) Synthesis and evaluation of chalcone derivatives as novel sunscreen agent. *Molecules*, **26**, 2698.
 26. Prachar, H., Chawla, A., Sharma, A. K., Kharb, R. (2012) Chalcone as a versatile moiety for diverse pharmacological activities. *International Journal Pharmaceutical Sciences and Research*, **3**, 1913–1927.
 27. Jamain, Z., Khairuddean, M. (2021) Synthesis and mesophase behaviour of benzylidene-based molecules containing two azomethine units. In *Proceedings of the Journal of Physics: Conference Series; IOP Publishing Ltd*, **1882**, 1882, 012120.
 28. Yeap, G. Y., Susanti, I., Teoh, B. S., Mahmood, W. A. K. (2005) Synthesis and phase transition in new chalcone derivatives: crystal structure of 1-phenyl-3-(4'-undecylcarbonyloxyphenyl)-2-propen-1-one. *Molecular Crystals and Liquid Crystals*, **442**, 133–146.
 29. Mandge, S., Singh, H. P., Gupta, D. S., Moorthy, N. H., S. N. (2007) Synthesis and characterization of some chalcone derivatives. *Trends in Applied Sciences Research*, **2**, 52–56.
 30. Moriya, K., Masuda, T., Suzuki, T., Yano, S., Kajiwara, M. (2006) Liquid crystalline phase transition in hexakis(4-(N-(4'-alkoxyphenyl)imino methyl)phenoxy) cyclotriphosphazene. *Molecular Crystals and Liquid Crystals*, **318**, 267–277.
 31. Jamain, Z., Khairuddean, M., Guan-Seng, T. (2020) Synthesis of new star-shaped liquid crystalline cyclotriphosphazene derivatives with fire retardancy bearing amide-azo and azo-azo linking units. *International Journal of Molecular Sciences*, **21**, 4267.
 32. Jamain, Z., Khairuddean, M., Guan-Seng, T. (2020) Liquid-crystal and fire-retardant properties of new hexasubstituted cyclotriphosphazene compounds with two Schiff base linking units. *Molecules*, **25**, 2122.
 33. Tsuji, T., Takeuchi, H., Egawa, T., Konaka, S. (2001) Effects of the molecular structure on the stability of a thermotropic liquid crystal. Gas electron diffraction study of the molecular structure of phenyl benzoate. *Journal of the American Chemical Society*, **123**, 6381–6387.
 34. Wan, W., Guang, W. J., Zhao, K. Q., Zheng, W. Z., Zhang, L. F. (1998) Calamitic organometallic liquid crystals with a terminal metal. Synthesis and liquid crystal properties of dicarbonylrodium (I) b-diketonate complexes. *Journal of Organometallic Chemistry*, **557**, 157–161.
 35. Jamain, Z., Azman, A. N. A., Razali, N. A., Makmud, M. Z. H. (2022) A review on mesophase and physical properties of cyclotriphosphazene derivatives with Schiff base linkage. *Crystals*, **12**, 1174.
 36. Abbasi, A. R., Rezvani, Z., Nejati, K. (2006) Synthesis and properties of new liquid crystalline compounds containing an alkoxyphenylazo group. *Dyes and Pigments*, **70**, 71–75.
 37. Jamain, Z., Khairuddean, M., Loh, M. L., Manaff, N. L. A., Makmud, M. Z. H. (2020) Synthesis and characterization of hexasubstituted cyclotriphosphazene derivatives with azo linking units. *Malaysian Journal of Chemistry*, **22**, 125–140.
 38. Jamain, Z., Khairuddean, M., Guan-Seng, T., Rahman, A. B. A. (2021) Synthesis, characterization and mesophase transition of hexasubstituted cyclotriphosphazene molecules with Schiff base and azo linking units and determination of their fire retardant properties. *Macromolecular Research*, **29**, 331–341.
 39. Thaker, B. T., Kanojiya, J. B. (2011) Synthesis, characterization and mesophase behavior of new liquid crystalline compounds having chalcone as a central linkage. *Molecular Crystals and Liquid Crystals*, **542**, 85–98.
 40. Shah, P., Soni, R., Soman, S. S. (2021) Synthesis and mesomorphic properties of bis ester derivatives of coumarin containing chalcone linkage. *Journal of Molecular Liquids*, **335**, 116178.